Experimental and Numerical Study of Solidification and Melting of Pure Materials

Satish P. Ketkar,* Masood Parang,† and Rao V. Arimilli†
University of Tennessee, Knoxville, Tennessee 37916

Solidification experiments in an enclosure are performed with caprillic acid as the phase-change fluid, and the experimental results for the temperature and solidification front advancement are presented. Caprillic acid, with its less than ambient melting point and low volume reduction on solidification, emerges as a good candidate for solidification experiments. An enthalpy formulation for convection/diffusion phase change in conjunction with an algorithm similar to SIMPLER is used in a formulation developed by Voller for solid-liquid phase change, to generate a numerical solution for low- and high-Prandtl-number fluids. The numerical solution is compared with solidification experimental data. In addition, the numerical solution is also compared with experimental melting data of Wolf and Viskanta for pure tin. The results indicate a good agreement between the experimental data and numerical solutions. This adds confidence to the formulation used in this numerical model.

Nomenclature

A = aspect ratio, height/length
c = specific heat of solid and liquid
D/Dt = substantial derivative
Fo = Fourier number, $= \alpha t/L^2$
$f(T)$ = function defined by Eq. (5)
H = total enthalpy, $= h + f(t)$; $h = cT$
h_m = cT_m
L = length
P = pressure
Pr = Prandtl number, $= \mu c/k$
Ra = Rayleigh number, $= g\beta(T_H - T_m)L^3/\alpha\mu$
Ra^* = modified Rayleigh number, $= [\beta g L^3 \lambda \rho^2/\omega k]Pr$
Ste = Stefan number, $= c(T - T_m)/\lambda$
T = temperature
T_m = melt temperature
t = time
(u,v) = (x,y) velocities
x,y = coordinate axes defined in Fig. 3
α = thermal diffusivity, $= k/\rho c$
β = coefficient of thermal expansion
λ = latent heat
μ = dynamic viscosity
ρ = density

Introduction

SOLID-LIQUID phase-change heat transfer problems are important in many situations of engineering interest such as casting metals, freezing foods, and storing latent heat thermal energy. A number of methods are available for solution of these problems, and a comprehensive review of them is available in Crank.[1] In most of the early work in this area, conduction was the only mode of heat transfer considered. Experiments have shown that natural convection in the liquid region may play a significant role in the nature and the extent of the phase-front movement.[2-4]

There are several studies dealing with the melting and solidification of materials that include natural convective motion in the liquid region.[5-7] One of the popular formulations is the enthalpy method, in which the solid-liquid phase front is eliminated from the calculations with the result that a fixed-grid solution methodology can be successfully employed. In a recent study by Voller et al.,[8] the enthalpy method was used in conjunction with the SIMPLE algorithm of Patankar[9] for the solution of mass, momentum, and energy equations. The main feature of this formulation is the isolation of the latent heat effects in the so-called source term. This makes the method amenable for use in the algorithm described by Patankar.[9] Exaggerated pressure corrections lead to a need for underrelaxation to avoid divergence in the SIMPLE algorithm. To eliminate the use of underrelaxation, the SIMPLER algorithm was developed by Patankar. In contrast to Ref. 8, which used the SIMPLE algorithm, in the present study a form of the SIMPLER algorithm is used. In the SIMPLER algorithm the energy equation is solved last in the iterative process, which works very well for solidification problems at earlier times because there is a strong driving potential for the natural convection flow. As time progresses, the convection flow decays and the algorithm stops iterating on velocities. To avoid these difficulties, a modified algorithm is used in this study and is presented and discussed in the next section. Brent et al.[10] have validated the method by comparing the numerical results with the melting experiments conducted by Gau and Viskanta.[4] The material used in the melting experiments was pure gallium with a melting point near room temperature (29.78°C).

In the present paper the authors have developed a computer code incorporating the technique by Voller et al.[8] in conjunction with a form of the SIMPLER algorithm. To validate the numerical code, two separate experimental data are used. First, the authors designed and performed experiments using 98% pure caprillic acid (melting point 14°C, $Pr = 81.17$). The experimental apparatus and the results will be explained in detail shortly. The data obtained on temperature history and phase-change front location in this experiment are used to verify the numerical results. Finally, experimental data from Wolf and Viskanta[11] for melting of pure tin (melting point 231.9°C, $Pr = 0.0089$) is used to verify further the validity of the numerical model for application in the melting process. After comparison of the numerical results with the experimental data, the validity of the numerical model is presented and discussed.

Received Oct. 3, 1988; revision received June 5, 1989.

*Graduate Student, Department of Mechanical Engineering.
†Professor, Department of Mechanical Engineering. Member AIAA.

Numerical Model

The following assumptions are used in conservation equations for the melt and the solid region. The thermophysical properties of the solid and liquid phases are assumed constant and equal. In addition, the melt is assumed to be an incompressible laminar Newtonian fluid, and the Boussinesq approximation is presumed to be valid. Using the following nondimensionalization:

$$x^* = \frac{x}{L}, \quad y^* = \frac{y}{L}, \quad u^* = \frac{u}{\alpha/L}, \quad v^* = \frac{v}{\alpha/L}$$

$$P^* = \frac{p}{\rho(\alpha/L)^2}, \quad Fo = \frac{\alpha t}{L^2}$$

$$T^* = \frac{T - T_m}{\lambda/c}, \quad H^* = \frac{H - H_m}{\lambda} \tag{1}$$

and dropping the superscript asterisk, the governing dimensionless equations for continuity and momentum reduce to

$$\frac{\partial u}{\partial x} + \frac{\partial v}{\partial y} = 0 \tag{2}$$

$$\frac{Du}{D(Fo)} = Pr[\nabla^2 u] - \frac{\partial p}{\partial x} \tag{3}$$

$$\frac{Dv}{D(Fo)} = Pr[\nabla^2 v] - \frac{\partial p}{\partial y} + Ra^* T \tag{4}$$

The main feature of the present methodology is the isolation of latent heat effects in the source term; i.e., $H = h + f(T)$, where

$$f(T) = \begin{cases} 1 & T > T_m \\ 0 \le f(T) \le 1 & T = T_m \\ 0 & T < T_m \end{cases} \tag{5}$$

Substituting this into the energy equation and noting that at the interface the velocity is zero, the energy equation reduces, in dimensionless form, to

$$\frac{\partial h}{\partial (Fo)} + \left(u\frac{\partial h}{\partial x} + v\frac{\partial h}{\partial y} \right) - \nabla^2 h + \frac{\partial f(T)}{\partial (Fo)} = 0 \tag{6}$$

This equation is similar to the general differential equation described by Patankar and can be solved by the methods described in Ref. 9. To make velocities approach zero in the control volumes undergoing phase change, Voller et al.[8] have proposed the addition of a large term, s, in the leading coefficient (Ap) of the momentum equations, where

$$s = \text{large term} \times [1 - \Delta f(T)]$$

In the liquid, $f(T) = 1$ and the value of s is 0, whereas in the solid, $f(T) = 0$ and s is equal to the large term. For control volumes undergoing a phase change, we have

$$0 < f(T) < 1$$

and s is between zero and the large term. This ensures a gradual slowdown of velocities in the control volumes changing phase and ensures that the velocities are very close to zero in the solid, whereas the velocity solution is unaffected in the liquid region. The method for dealing with $f(T)$ during the solution iterations of the SIMPLER algorithm is discussed in detail elsewhere.[8] A brief description of the method follows.

On commencement of the SIMPLER algorithm over one time step, initial values for current nodal latent heats are taken to be the values at the previous time level. After solution of nodal enthalpies at the ith iteration, $f(T)$ is updated in the following way:

$$[f(T)]_{i+1} = f(T)_i + (h)_i$$

and if

$$[f(T)]_{i+1} > 1 \quad \text{set} \quad [f(T)]_{i+1} = 1$$

or if

$$[f(T)]_{i+1} < 0 \quad \text{set} \quad [F(T)_{i+1} = 0]$$

After the ith iteration cycle of SIMPLER is complete, the front is within those control volumes for which $0 < f(T) < 1$, and its precise location can be found by the value of $f(T)$ [e.g., $f(T) = 0.6$ means the control volume is 60% liquid]. Another way to get the front location is by examining isotherms where the front is associated with the isotherm with the zero value. The major advantage of the enthalpy formulation is that a fixed-grid numerical formulation can be employed, and the energy balance condition at the interface is automatically satisfied. The limitation of enthalpy method (weak method) is that it does not specifically account for discontinuities in the problem and therefore is not very accurate near the region of discontinuity. A more detailed discussion of the method used can be found in Refs. 8 and 10.

Equations (2–6) are solved by the SIMPLER-like algorithm[9] in conjunction with the enthalpy-porosity technique proposed by Voller et al.[8] In order to avoid difficulties arising from decaying convection and melting at small times, the following algorithm is used: The solution is started with an assumed velocity field. With this assumed value the energy equation is solved to generate temperature solution. The coefficients of the momentum equation are then computed. The coefficients of pressure equation are calculated next, and the pressure field is determined. The momentum equations are then solved using this pressure field. Conservation of mass is checked at this point, and, if mass conservation is not satisfied, then the pressure correction equation is solved. The velocity field is then corrected using the pressure corrections. With the newly corrected velocity field, the energy equation is now solved, and the process is repeated until the continuity equation is satisfied. The algorithm is then advanced in time.

Grid refinement studies were conducted for determining the level of accuracy of the numerical solution. Table 1 illustrates the effect of varying grid size on volume fraction, temperature, and CPU for a selected case ($Pr = 1$, $Ra^* = 10^5$, $Fo = 0.063$, $T_c = -0.5$, $T_i = 0.5$). It is observed that with the use of a finer grid the time step needs to be reduced to achieve convergence. Therefore, for a given Fourier number, the computation time is increased not only due to a large number of grid points but often also due to the necessity of choosing a substantially larger number of required time steps. The refinement of the grid size was terminated when the volume fraction solidification results were observed to level off (40×40 in this case). Similar results were obtained for other Prandtl and Rayleigh numbers, e.g., 10 and 5.17×10^9, respectively, $A = 2.3$, and $Fo = 0.01$. In addition, it was found that, for a given Rayleigh number and time step, reducing the Prandtl number results in slower convergence. Similarly, increasing the Rayleigh number with a fixed Prandtl number and time step increases the required CPU time. In addition, convergence is not achieved beyond a certain Rayleigh number (different for each case) without reducing the time step.

The preceding grid refinement analysis and the prohibitive cost of computational time for very fine mesh size (up to two orders of magnitude more) suggested a 12×22 mesh size for the freezing case and a 15×15 mesh size for the melting case.

Table 1 Influence of grid size on computed results for $Pr = 1$, $Ra^* = 10^5$, $Fo = 0.063$, $T_c = -0.5$, and $T_i = 0.5$

Grid	Volume fraction solidification	Temperature ($X = 1$, $Y = 1.0$)	ΔFo	CPU time
8×8	0.114	0.31	0.01	1 min
15×15	0.121	0.410	0.001	7 min
20×20	0.129	0.435	0.001	20 min
30×30	0.137	0.4499	0.0001	1.5 h
40×40	0.136	0.4553	0.0001	3 h

The selection was made based on both a reasonable CPU time and a numerical deviation limited to 10% or less compared with the finest mesh size shown in Table 1.

The flow structure for the test case (40×40 grid) is shown in Figs. 1 and 2. It can be seen that no secondary flow is predicted in the flowfield for this configuration. Similarly, no secondary flow is observed at higher Ra^* (up to $Ra^* = 10^9$ was computed). Other researchers using an enthalpy technique[5,10] for the convection-diffusion melting problem also have not reported any recirculating cells. However, using a temperature-based stream-function formulation, Ramachandran et al.[7] observed recirculating flow near the corners for a solidification problem even with a crude mesh size (10×10 in. solid and liquid region).

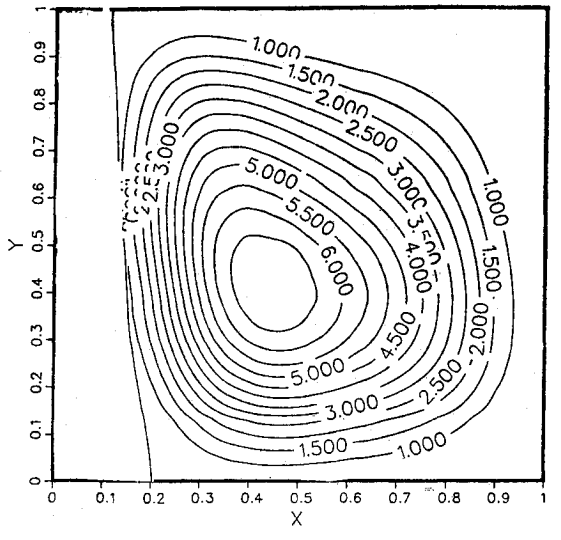

Fig. 1 Streamlines at $Fo = 0.063$ ($Pr = 1$, $Ra^* = 10^5$, 40×40 grid).

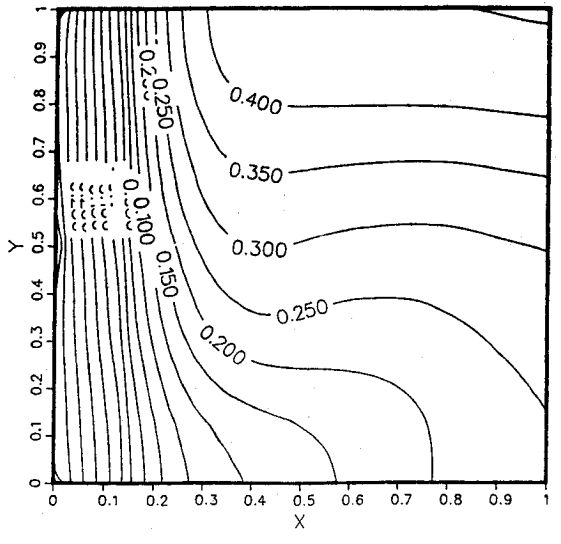

Fig. 2 Isotherms at $Fo = 0.063$ ($Pr = 1$, $Ra^* = 10^5$, 40×40 grid).

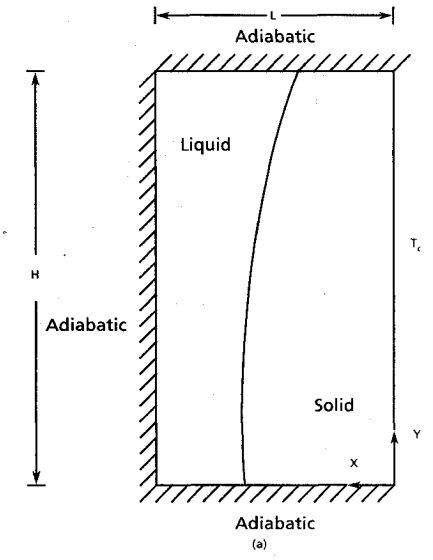

Fig. 3a Coordinate system and boundary conditions.

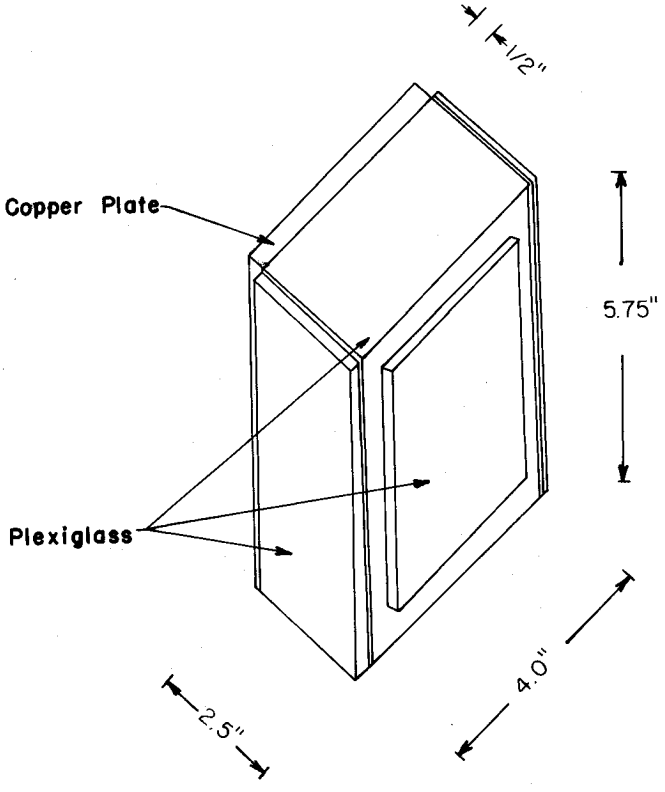

Fig. 3b Schematic of the experimental setup.

Experiment

Solidification experiments are conducted in a rectangular enclosure to simulate a two-dimensional freezing. One wall of the enclosure is made of two ¼-in. copper plates that are joined together with screws. Cold water from an ice-water solution is circulated through internal milled passages between the copper plates using a pump. In this study the copper wall is maintained at 3°C, which is 11°C below the freezing temperature of the caprillic acid. Figure 3 shows the schematic of the experimental apparatus designed and built for this study. In addition to the copper wall (cold wall), the enclosure is comprised of five walls made of ¾-in. Plexiglas (adiabatic walls). Plexiglas is used because of its low thermal conductivity and to make possible the visualization of the freezing front. Based on the previously reported successful experimental setups,[3,4] an experimental apparatus with an aspect ratio of 2.3 was de-

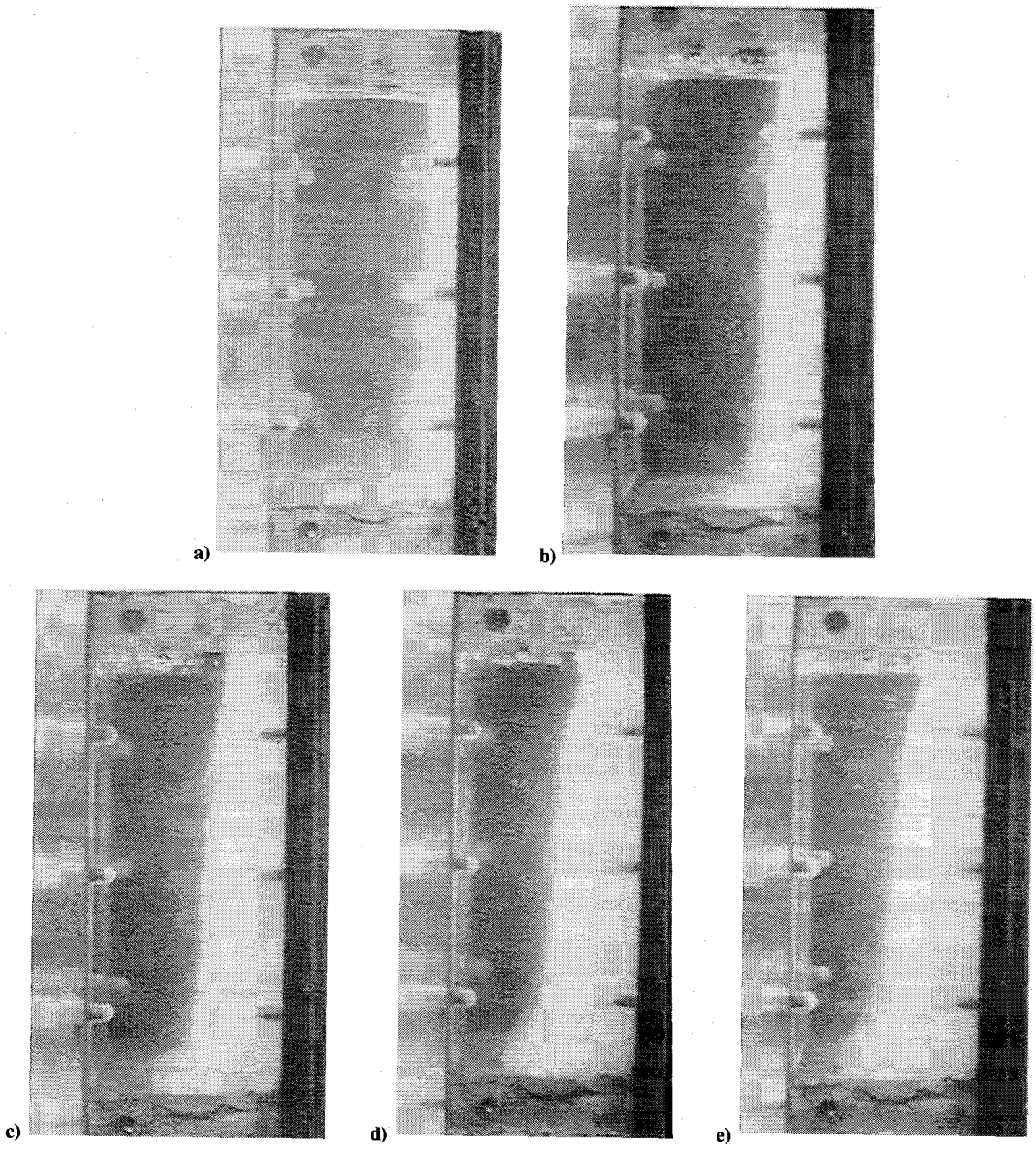

Fig. 4 Solid-liquid interface location at a) 1 h, b) 2 h, c) 4 h, d) 6 h, e) 7 h.

signed and constructed (Fig. 3) to provide a two-dimensional flowfield. As will be described shortly, the results confirmed the two-dimensional nature of the flow.

Caprillic acid was chosen as the working fluid in the experiments because it has a melting point of 14°C and a small volume change when solidified (3–4%). The main advantage of caprillic acid is that its melting point is typically only a few degrees below the ambient room conditions, which provides convenience in the design of the experimental setup. The thermophysical properties of caprillic acid are well established and can be found in Ref. 12. Finally, although the material used has a small impurity of 2%, no dendritic structure was observed. Furthermore, the phase front was observed to remain sharp, indicating that the phase change occurs at a fixed temperature within the experimental uncertainty.

The phase front is easily visualized through the Plexiglas sidewalls, and its advancement is directly measured (with an uncertainty of 1 mm) and at the same time photographed using an SLR camera (Fig. 4). It was observed that, except in a region very close to the sidewalls (within 2% of the enclosure width), no deviation from two-dimensionality occurs in the main remaining core section of the enclosure. This is clearly confirmed by the shape of the solid-liquid interface observed throughout the experiment. Temperature measurement was carried out at two locations. One was at $x = 1.02$ cm (0.4 in.) and $y = 7.62$ cm (3.0 in.) and the other at $x = 5.08$ cm (2.0 in.) and $y = 7.62$ cm (3.0 in.). The latter location remained in liquid state throughout the experimental run of 3.5 h. The thermocouple used to measure the temperature was mounted on a 2-mm-diam low-thermal-conductivity ceramic rod and was inserted in the experimental setup through a small aperture at the top of the enclosure.

Results and Discussion

Freezing Case

The numerical solution developed in this study is compared with caprillic acid solidification experiments conducted for this specific purpose and is discussed in the previous section. Caprillic acid properties used in the model include the following: thermal conductivity 0.148 W/m-K, coefficient of thermal expansion 9×10^{-4}1/K, density 910 kg/m^3, dynamic viscosity 5.74×10^{-3} kg/m-s, specific heat 2093 J/kg-K, and latent heat 1.49×10^5 J/kg. The parameters for this experiment include the following: $Ra = 5.17 \times 10^9$, $Ste = 0.187$, $Pr = 81.17$, and

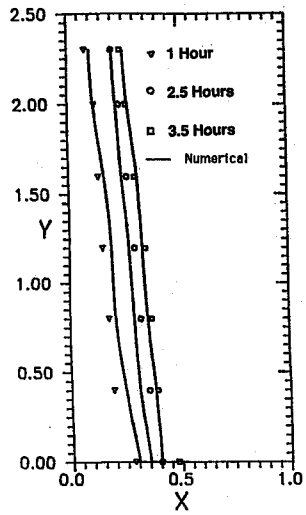

Fig. 5 Comparison of the numerical and experimental solidification fronts of caprillic acid ($T_w = 3°C$, $Ra^* = 5.17 \times 10^9$).

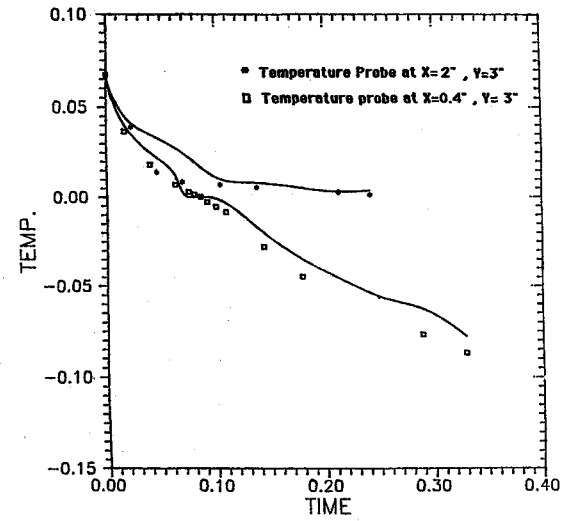

Fig. 6 Numerical and experimental temperature results for solidification of caprillic acid ($T_w = 3°C$, $Ra^* = 5.17 \times 10^9$).

$A = 2.3$. A numerical grid of 12×22 is employed. For the melting experiments there is a characteristic temperature difference, which is used in normalizing the temperature field. For the solidification experiments, however, there was no characteristic driving temperature difference for the natural convection flow, therefore, a ratio of latent heat to specific heat [as described in Eq. (1)] was used. The phase-front location computed numerically and measured experimentally is shown in Fig. 5. The numerical solution and experimental results are in good agreement. There is a discrepancy between the two solutions near the bottom of the enclosure. Specifically, the experiments show a "toe" at the bottom of the phase-front profile. This may be due to the insignificant but present heat loss through the bottom wall which is ignored in the numerical model. In addition, conduction along the walls (ignored in the numerical model) may, when coupled with the direction of the convection cell in the melt, be responsible for the observed toe near the bottom wall.

Figure 6 shows numerical and experimental comparison of temperature solutions at two locations. One of the points goes through the change of phase, whereas the other stays in the liquid region for the duration of this particular experimental run of 3.5 h. The experimental and numerical solutions agree well at later times. At earlier times the numerical solution appears to predict weaker natural convection than that shown by the experimental data. This is believed to cause the discrepancy in the experimental and numerical temperature results at small times. The Rayleigh number for the solidification experiment is of the order of 10^9, which required a time step of 10^{-4} to achieve convergence at each time step. The CPU time for the longest solidification run was 2.05 h.

Melting Case

The numerical code developed generated results for the interface locations at various times. Specifically, the code was run for melting of pure metal tin in a rectangular enclosure, and the results are compared with the experimental data of Wolf and Viskanta[11] for $Ra = 2.91 \times 10^5$, $Ste = 8.48 \times 10^{-3}$, $Pr = 0.0089$, and $A = 0.75$. The numerical simulation was continued up to a real time of 2.089 h ($Fo = 16.75$). The results are compared for 0.579, 1.012, and 2.079 h. The numerical code was run with 15×15 grid on a VAX 8800 computer. The numerical code employed in this study was run with a time step of 10^{-3}. CPU time for the longest melting run was 15 min. At each time step the energy balance was checked by comparing the difference in energy in the system over a time step with the energy taken out (or put in as the case may be) from the cold (or hot) wall. Finally, the global energy balance was checked at the end of each computational run to guarantee compliance.

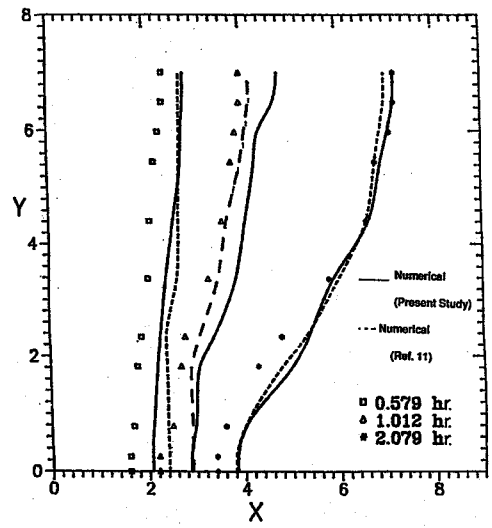

Fig. 7 Comparison of the numerical and experimental interface locations for melting of pure tin, at 0.579, 1.012, and 2.079 h ($T_w = 233.9°C$, $\Delta T = 2°C$, $Ra = 2.91 \times 10^5$).

The numerical and experimental results for front locations in melting experiments are shown in Fig. 7. The solid lines represent the numerical solution of the present study, and the dashed lines represent the numerical solution from Ref. 11. At 0.579 and 1.1012 h the numerical solution overpredicts the experimental observations. The discrepancy at 0.579 h is 10% at $y = 0.75$ and 12% at $y = 0$ for the present study, whereas it is about 8.6% at $y = 0.75$ and 22% at $y = 0$ for the numerical study of Wolf and Viskanta.[11] Both numerical results have a large (20%) discrepancy at short times (e.g., 1.012 h) at the bottom ($y = 0$) of the enclosure. The present computed solution has a difference of approximately 12% with experimental data at 2.079 h near the bottom of the enclosure. The discrepancy between the numerical and experimental data at earlier times may be explained by the thermal inertia of the experimental system.[11] Wolf and Viskanta have used the method described by Webb and Viskanta[12] to compare their results. This method employs a front tracking scheme and uses temperature as the independent variable. The use of enthalpy method in the present study eliminates the need to track the phase front at each time step.

Numerical and experimental results for the temperature at a real time of 2.079 h in the melting experiment are shown in Fig. 8 for $A = 0.9$ and $A = 0.1$. The solid line represents the numerical solution of the present study, and the dashed lines

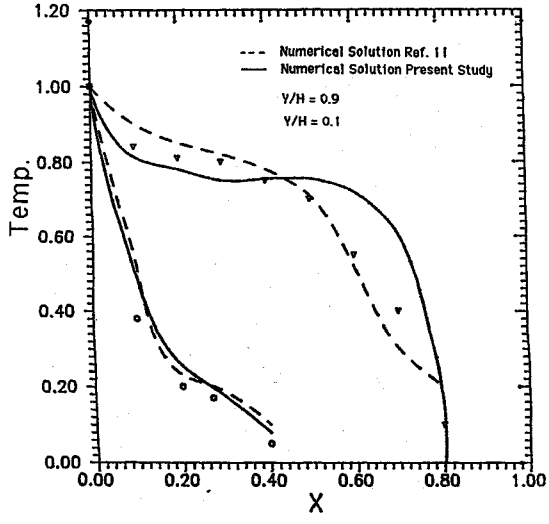

Fig. 8 Comparison of the numerical and experimental temperature measurement for melting of pure tin ($T_w = 233.9°C$, $\Delta T = 2°C$, $t = 2.079$ h).

represent the numerical solution of Ref. 11. The computed temperature solutions at the top of the enclosure ($A = 0.9$) show a large discrepancy with the experimental data. The experimental and numerical solutions, however, are in better agreement near the bottom of the enclosure ($A = 0.1$). Convection is pronounced in the positive x direction at the top of the enclosure for the melting problem, and it transports the thermal energy up to the melt front, where the dimensionless temperature is zero. This results in high-temperature gradients in the vicinity of the melt front, which are confirmed by the experimental data. The present numerical model used in this study overpredicts this behavior.

Conclusions

An enthalpy formulation, isolating the latent heat effects in the source term, is used for the convection/diffusion phase-change processes. The numerical solution is compared with the experimental data for the solidification of caprillic acid and the melting of tin. The numerical predictions and experimental results are in good agreement for the phase-front locations and reasonable agreement for temperature-time history. The results suggest confidence in the developed numerical scheme. Caprillic acid, with its less than ambient melting point and low volume reduction, proves to be a good candidate for solidification experiments.

References

[1]Crank, J., *Free Moving Boundary Problems,* Clarendon, Oxford, UK, 1984, Chaps. 3-6.

[2]Sparrow, E. M., Ramsey, J. W., and Kemink, R. G., "Freezing Controlled by Natural Convection," *Journal of Heat Transfer,* Vol. 101, No. 4, 1979, pp. 578-584.

[3]Hale, N. W., Jr., and Viskanta, R., "Solid-Liquid Phase-Change Heat Transfer and Interface Motion in Materials Cooled or Heated From Above or Below," *International Journal of Heat and Mass Transfer,* Vol. 23, No. 3, 1980, pp. 283-292.

[4]Gau, C., and Viskanta, R., "Melting and Solidification of a Metal System in a Rectangular Cavity," *International Journal of Heat and Mass Transfer,* Vol. 27, No. 1, 1984, pp. 113 123.

[5]Schneider, G. E., "Computation of Heat Transfer with Solid/Liquid Phase Change Including Free Convection," *Journal of Thermophysics and Heat Transfer,* Vol. 1, No. 2, 1987, pp. 136-145.

[6]Gartlin, D. K., "Finite Element Analysis of Convective Heat Transfer Problems With Change of Phase," *Computer Methods in Fluids,* edited by K. Morgan, C. Taylor, and C. A. Brebbia, Pentech, London, 1980, pp. 257-284.

[7]Ramachandran, N., Gupta, J. P., and Jaluria, Y., "Thermal and Fluid Flow Effects During Solidification in a Rectangular Enclosure," *International Journal of Heat and Mass Transfer,* Vol. 25, No. 2, 1982, pp. 187-194.

[8]Voller, V. R., Cross, M., and Markatos, N. C., "An Enthalpy Method of Convection-Diffusion Phase-Change," *International Journal for Numerical Methods in Engineering,* Vol. 24, No. 1, 1987, pp. 271-284.

[9]Patankar, S. V., *Numerical Heat Transfer and Fluid Flow,* Hemisphere, Washington, DC, 1980.

[10]Brent, A. A., Voller, V. R., and Reid, K. J., "Enthalpy-Porosity Technique for Modeling Convection-Diffusion Phase-Change: Application to Melting of a Pure Metal," *Numerical Heat Transfer,* Vol. 13, No. 3, 1988, pp. 297-318.

[11]Wolf, F., and Viskanta, R., "Melting of a Pure Metal From a Vertical Wall," *Experimental Heat Transfer,* Vol. 1, No. 1, 1987, pp. 17-30.

[12]Webb, B. W., and Viskanta, R., "Analysis of Heat Transfer During Melting of a Pure Metal from an Isothermal Vertical Wall," *Numerical Heat Transfer,* Vol. 9, No. 1, 1986, pp. 539-558.

[13]Markley, K. S. (ed.), *Review: Fatty Acids, Part 1,* 2nd ed., Interscience, New York, 1960, pp. 34-38.